Microfluidically supported biochip design for culture of endothelial cell layers with improved perfusion conditions



2015 Biofabrication 7 015013

(http://iopscience.iop.org/1758-5090/7/1/015013)

Biofabrication

PAPER

# Microfluidically supported biochip design for culture of endothelial cell layers with improved perfusion conditions

RECEIVED
17 September 2014

REVISED
15 January 2015

ACCEPTED FOR PUBLICATION
28 January 2015

PUBLISHED
2 March 2015

**Martin Raasch**[1,7], **Knut Rennert**[1], **Tobias Jahn**[4], **Sven Peters**[2], **Thomas Henkel**[3], **Otmar Huber**[1,7], **Ingo Schulz**[4], **Holger Becker**[4], **Stefan Lorkowski**[5], **Harald Funke**[6] **and Alexander Mosig**[1,7]

[1] Institute of Biochemistry II, Jena University Hospital, Nonnenplan 2-4, D-07743 Jena, Germany
[2] Department of Ophthalmology, Jena University Hospital, Bachstraße 18, D-07743 Jena, Germany
[3] Institute of Photonic Technology (IPHT), Albert Einstein Straße 9, D-07745 Jena, Germany
[4] microfluidic ChipShop GmbH, Stockholmer Straße 20, D-07747 Jena, Germany
[5] Institute of Nutrition, Friedrich Schiller University Jena, Dornburger Str. 25, D-07743 Jena, Germany
[6] Molecular Hemostaseolgy, Jena University Hospital, Bachstraße 18, D-07743 Jena, Germany
[7] Center for Sepsis Control and Care, Jena University Hospital, Erlanger Allee 101, D-07747 Jena, Germany

**E-mail:** alexander.mosig@med.uni-jena.de

**Keywords:** endothelial cells, microfluidic, dynamic cell culture

Supplementary material for this article is available online

## Abstract

Hemodynamic forces generated by the blood flow are of central importance for the function of endothelial cells (ECs), which form a biologically active cellular monolayer in blood vessels and serve as a selective barrier for macromolecular permeability. Mechanical stimulation of the endothelial monolayer induces morphological remodeling in its cytoskeleton. For *in vitro* studies on EC biology culture devices are desirable that simulate conditions of flow in blood vessels and allow flow-based adhesion/permeability assays under optimal perfusion conditions. With this aim we designed a biochip comprising a perfusable membrane that serves as cell culture platform multi-organ-tissue-flow (MOTiF biochip). This biochip allows an effective supply with nutrition medium, discharge of catabolic cell metabolites and defined application of shear stress to ECs under laminar flow conditions. To characterize EC layers cultured in the MOTiF biochip we investigated cell viability, expression of EC marker proteins and cell adhesion molecules of ECs dynamically cultured under low and high shear stress, and compared them with an endothelial culture in established two-dimensionally perfused flow chambers and under static conditions. We show that ECs cultured in the MOTiF biochip form a tight EC monolayer with increased cellular density, enhanced cell layer thickness, presumably as the result of a rapid and effective adaption to shear stress by remodeling of the cytoskeleton. Moreover, endothelial layers in the MOTiF biochip express higher amounts of EC marker proteins von-Willebrand-factor and PECAM-1. EC layers were highly responsive to stimulation with TNF$\alpha$ as detected at the level of ICAM-1, VCAM-1 and E-selectin expression and modulation of endothelial permeability in response to TNF$\alpha$/IFN$\gamma$ treatment under flow conditions. Compared to static and two-dimensionally perfused cell culture condition we consider MOTiF biochips as a valuable tool for studying EC biology *in vitro* under advanced culture conditions more closely resembling the *in vivo* situation.

## Introduction

Endothelial cells (ECs) lining the inner lumen of blood vessels form a barrier for ions, nutrients, water and macromolecules and are responsible for important homeostatic functions such as the regulation of the vessel tonus or coagulation by secretion of bioactive molecules. Endothelial layers are also important regulators of vascular inflammation due to their ability to recruit immune cells from the circulation via expression of cell adhesion molecule (CAM) in response to tissue damage or infection. Shear stress is a critical factor for endothelial function as mechanic stimulation of the EC membrane has been demonstrated to mediate morphological adaptations (Flaherty *et al* 1972, Davies *et al* 1976, Goode *et al* 1977), and

to regulate endothelial permeability (Kwei *et al* 2004). Moreover, shear stress is involved in the regulation of inflammatory reactions at the onset of cardiovascular diseases such as atherosclerosis (Traub and Berk 1998).

Endothelial adaption to dynamic cell culture under flow conditions includes the modulation of the cytoskeleton in response to shear stress. F-actin microfilaments have been shown to reorganize under flow conditions into long, dense stress fibers crossing the cells in a direction perpendicular to flow. During this process the cytoskeleton forms bridges between mechanosensors on the luminal apical side and the integrins on the basal side, which also have been described as mechanotransducers (Davies 1995, Geiger *et al* 2001). One of these sensors is the platelet endothelial cell adhesion molecule-1 (PECAM-1), the major constituent of the EC intercellular junctions which has been shown to transmit mechanical forces via PI3K/Akt-mediated integrin activation and actin microfilament alignment (Tzima *et al* 2005). Beyond, PECAM-1 is involved in the maintenance of endothelial integrity preserving barrier function and preventing alterations of the cellular environment that could contribute to organ dysfunction (Harhaj and Antonetti 2004). In addition, shear stress has been reported to regulate expression of CAMs and to modulate monocyte adhesion to the vascular endothelium. Under flow conditions cell surface expression of intercellular adhesion molecule-1 (ICAM-1) is selectively up-regulated (Nagel *et al* 1994), whereas expression of vascular cell adhesion molecule-1 (VCAM-1) and E-selectin is reported to be decreased in response to shear stress (Chiu *et al* 2004).

*In vitro* studies in EC biology rely on reproducible culture conditions that resemble critical parameters of the *in vivo* state. Microfluidically supported flow chambers have emerged as advanced tools for EC culture within the last decade. Micro-scaled flow chambers offer the advantages of low consumption of reagents and biological samples, a high flexibility in the design of integrated structures, and optimal control of cell patterning (El-Ali *et al* 2006, Whitesides 2006, Wang *et al* 2011). Established two-dimensionally perfused flow chambers mostly comprise rhombic shaped cavities with a tight bottom serving as cell culture area that is perfused with cell culture medium under laminar flow conditions. However, these two-dimensionally perfused flow chambers provide only the option of apical perfusion and therefore lack the opportunity for flow-based studies on permeability or investigations of e.g. cytokine actions on the basal cell membrane during dynamic culture.

The vast majority of flow chambers used for the culture of EC layers is based on polydimethylsiloxane (PDMS) due to its ease of use for a rapid manufacturing of prototypes (Young and Simmons 2010). PDMS is biological compatible, transparent and exibits low autofluorescence which makes it suitable for on-chip fluorescence microscopy (Berthier *et al* 2012). However, elastic PDMS possess a couple of drawbacks, e.g. hydrophobic molecules can adsorb to the bulk of the PDMS and uncrosslinked monomers tend to migrate from the bulk to the surface, allowing to recover surface hydrophobicity even after oxygen plasma treatment (Eddington *et al* 2006, Toepke and Beebe 2006). Uncrosslinked PDMS monomers have also been found to leach out from the bulk, into the media and affecting cellular behavior (Regehr *et al* 2009). Furthermore, PDMS is permeable to gases and water vapor, causing changes in the osmolarity of the cell culture medium (Thuenauer *et al* 2014).

We designed a chip architecture that uses porous membranes as also utilized in Transwell filter inserts serving as cell culture substrate (Ramello *et al* 2011, Huh *et al* 2013, Jang *et al* 2013, Ramadan *et al* 2013) allowing apical and basolateral perfusion of EC layers in parallel during cell culture within the biochip. Cyclic olefin copolymers (COCs) have been used for manufacturing of cell culture devices to overcome limitations of PDMS. COCs do not unspecifically absorb medium contents and bulk surfaces of biochips can easily been functionalized by long lasting plasma treatment for hydrophilization. Furthermore COC possess high stability, ideal optical characteristics for bright field as well as fluorescence microscopy and is frequently used in medical devices due to its proven biocompatibility (van Midwoud *et al* 2012). For the first time, we here systemically characterize and compare the impact of the different cell culture methods of expression on endothelial marker proteins and cell growth under static and dynamic conditions in established two-dimensionally perfused flow chambers and MOTiF biochips to proof the benefits of EC culture within membrane-containing biochips.

## Methods

### HUVEC and THP-1 cells

ECs were isolated from human umbilical cord veins (HUVEC) as described elsewhere (Jaffe *et al* 1973). Donors were informed about the aim of the study and gave written informed consent. The study was approved by the ethics committee of the Friedrich-Schiller-University Jena, Germany. Experiments were performed with HUVEC cells up to passage four cultured in EC medium (Promocell, Heidelberg, Germany). THP-1 cells were obtained from DSMZ (Braunschweig, Germany) and cultured in RPMI 1640 supplemented with 10% FCS (Life Technologies, Karlsruhe, Germany).

### Multi-organ-tissue-flow (MOTiF) biochip fabrication and surface treatment

MOTiF biochips and flow chamber chips were manufactured by and obtained from microfluidic ChipShop GmbH (Jena, Germany). The microfluidic devices

were made from Topas®, a COC. The chip was manufactured by injection molding using a modular mold base with exchangeable metallic mold inserts. The mold inserts were structured using ultra-precision mechanical machining using a 100 $\mu$m diameter machining bit for the smallest features and finishing. As first fabrication step the microstructured part with microfluidic channels network, fluidic interfaces and the area for membrane integration are made by injection molding. Afterwards the integration of the 11 $\mu$m thick polyethylene-terephthalate (PET) membrane with a pore diameter of 8 $\mu$m and a pore density of $2 \times 10^5$ pores/cm$^2$ (TRAKEDGE Sabeu, Radeberg, Germany) was carried out. The parts were then sealed on top and bottom side with an extruded 140 $\mu$m thick COC film using a low-temperature proprietary bonding method.

Surface oxidation for hydrophilization was accomplished by treatment with oxygen plasma using a T200G plasma generator (PVA Tepla AG, Wettenberg, Germany). The surface of the 2D perfusion chamber was oxidized as described for MOTiF chips. COC foils used for sealing in both chip designs show significant oxygen permeability. Gas permeable silicon tubing was used for two- and three-dimensional (3D) perfusion allowing oxygen equilibration during experimentation. Ramping structures have been introduced in the biochip design between membrane and membrane framing of the bulk to avoid unfavorable flow conditions and trapping of stationary bubbles. Bubble formation was reduced by oxygen plasma treatment of the whole chip surface and perfusion medium was stirred and equilibrated over night under perfusion conditions before use.

**Meassurement of contact angles**

Measurement of contact angles was done on injection-molded biochips without usage of any mold release agents. Contact angles were measured using a Dino-Lite AD4113TL (Long Working Distance) microscope camera and analyzed with the Dino Capture 2.0 software.

**Antibodies, flow cytometry and vitality stain**

The following antibodies were used for immunofluorescence microscopy: anti-CD31 (CellSignaling, MA, USA), anti-von Willebrand factor (vWF) (DAKO, Hamburg, Germany), anti-zonula occludens-1 (ZO-1), goat-anti-mouse-Cy3, goat-anti-rabbit-AF488 (Life Technologies), and goat-anti-rabbit-AF647 (Dianova, Hamburg, Germany). Actin was stained with phalloidin-AF633 (Life Technologies). Immunofluorescence microscopy was performed with Axio Observer Z1 (Zeiss, Jena) controlled by AxioVision 4.8.2 software (Zeiss, Jena). Z-stack imaging was done with a Zeiss LSM 710 confocal microscope (Zeiss, Jena, Germany). Fluorescence analysis, quantification of immunofluorescence staining and cell shape analysis was performed with ImageJ 1.46r. Calcein-AM (Life Technologies)-staining was performed according to manufacturer's recommendations. For flow cytometry the antibodies anti-CD31-FITC, anti-CD62e-PECy5, anti-CD106-V450 (BD Pharmingen, Heidelberg, Germany), anti-CD54-AF647 (BioLegend, San Diego, CA, USA) and isotype control antibodies mouse IgG1-FITC, mouse IgG1-PE (Miltenyi Biotec, Bergisch-Gladbach, Germany), mouse IgG1-APC (BioLegend), mouse IgG1-PECy5 and rat IgG2a-eFluor450 (eBioscience, San Diego, CA, USA) were used. Flow cytometry was done using a BD FACS-Canto™ II (BD BioScience, Heidelberg, Germany) and data were analyzed with FlowJo v7.6.5 (TreeStar, Ashland, OR, USA).

**Computational fluid dynamic (CFD) simulations**

CFD simulations were performed using the OpenFOAM CFD-toolkit (the OpenFoamFoundation, http://www.openfoam.org) in combination with the ParaView Toolkit (Henderson 2004) for data visualization and analysis. Surface triangulated meshes were obtained from the geometry models using the gmsh utility (Geuzaine and Remacle 2009). Volume hexaeder meshes were generated using the snappyHexMesh utility of OpenFoam. Transient simulations have been performed using the interFoam solver as provided by OpenFOAM Version 2.2.0 for a flow rate of 20 $\mu$l s$^{-1}$. with aqueous phase Reynolds number Re of 28 in the inflow and outflow cylinders, Re of 12 in the inflow section of the main chamber and Re of 5.5 in the main section of the chamber. Time step size was adjusted dynamically to a fluid and interface Courant number below 0.15. Final tolerance limits were set in the fvSolution parameter dictionary of the solver to 1 10-9 for the p_rghFinal iterations and to 1 10-10 for the UFinal iterations. Interface compression defined by the parameter cALPHA was switched off by setting the value to zero.

**Flow culture experiments**

Microfluidic cell culture experiments were performed under a specialized clean bench for microfluidic applications with environment control of 5% $CO_2$, 70% air humidity and 37 °C under sterile cell culture conditions (Automated Lab Solutions GmbH, Jena, Germany). HUVECs were seeded on MOTiF biochips and flow chambers with a density of $1.3 \times 10^5$ cells/cm$^2$. Static cell culture was performed in 24 well plates with 13 mm glass coverslips (Menzel, Braunschweig, Germany). Cells were cultured for 72 h until reaching confluence. Medium was changed on a daily basis in the wells or chips. ECs were cultivated under static conditions within the chips until reaching confluence. Chips then were perfused with medium using peristaltic pumps (Ismatec REGLO digital MS-CA-4/12-100, Wertheim, Germany). Shear stress of 0.7 and 10 dyn cm$^{-2}$ was applied for 24 h.

### Calculation of shear stress levels

Shear stress was calculated with the equation:

$$\tau = \frac{2^{\star}\mu^{\star}Q}{w^{\star}h^2}{}^{\star}\left(\frac{m+1}{m}\right)^{\star}(n+1)$$

( $\tau$: shear stress, $h$: height and $\omega$: width of the microfluidic chamber, $Q$: flow rate of the medium ). The values for $m$ and $n$ are empirical constants with $m = 1.7 + 0.5^{\star}\alpha^{-1.4}$ , and $n = 2$ for $\alpha < 1/3$ , where cross sectional aspect ratio $\alpha = h/w$ with $0 \leqslant \alpha \leqslant 1$ (Young and Simmons 2010).

### Permeability assay

EC were treated with 20 ng ml$^{-1}$ TNF$\alpha$ (Calbiochem, Billerica, MA, USA) and 10 ng ml$^{-1}$ IFN$\gamma$ (Peprotech, Hamburg, Germany) through the lower perfusion channel. After cytokine treatment endothelial layers were incubated with 10 mg ml$^{-1}$ of FITC-dextran for 30 min under static conditions. FITC-dextran that permeates through the layer was collected via the lower perfusion channel and analyzed with an iEMS Reader MF & Multiskan and Ascent Software version 2.6 (Thermo Scientific, Waltham, MA, USA).

### THP-1 adhesion assay

THP-1 cells were labeled with 1 $\mu$M CellTracker green CMFDA (Life Technologies, Karlsruhe, Germany). EC layers were perfused at the apical cell membrane via the upper perfusion channel with indicated shear stress and simultaneously stimulated at the basal cell membrane with 20 ng ml$^{-1}$ TNF$\alpha$ perfused via the lower perfusion channel of the MOTiF biochips through membrane pores with 8 $\mu$m diameter for 24 h. Within the last 30 min of the experiment EC layers were simultaneously perfused at the apical side with $2 \times 10^6$/(ml $\times$ h) labeled THP-1 using a neMESYS syringe pump with stirring module (Cetoni, Korbußen, Germany). After flushing with PBS, the cell layers were fixed for 10 min with 4% PFA (Sigma-Aldrich, MO, USA), mounted and nuclei were stained with DAPI (Life Technologies) and samples were mounted in fluorescent mounting medium (DAKO). THP-1/HUVEC ratio was calculated by counting labeled adherent THP-1 cells and DAPI stained HUVEC.

### Cell shape index (CSI) analysis

CSI analysis was performed by fluorescence staining of the CD31 membrane protein to locate cellular boundaries, analyzed with ImageJ and calculated using the formula $\mathrm{CSI} = 4\pi^{\star}\frac{A}{p^2}$ ($P$: cellular perimeter, $A$: area) (Malek and Izumo 1996). CSI defines cellular morphological shape ranging from 0 corresponding to circular shape to 1 corresponding to a straight line.

### Statistical analysis

All results are reported as average of the performed experiments with standard deviation. Where indicated multiple comparison analysis was performed using one-way-ANOVA testing with Tukey's multiple testing. Direct comparison of two conditions was done with two-tailed, non-paired Student's t-test. Statistical analysis was performed using GraphPad Prism 6 software (Graphpad Software, La Jolla, CA, USA).

## Results

Microfluidic chips are a promising tool to investigate endothelial layers and their interaction with immune cells. Here, we developed a microfluidically supported biochip, allowing a 3D perfusion of EC layers under defined shear stress conditions thereby providing enhanced nutrition supply and preventing enrichment of catabolic metabolite. To prove that the design of the MOTiF biochip allows culture of EC layers under conditions that resemble the natural situation we analyzed cell morphology, EC marker protein expression and functional responsiveness to chemokines and compared it with established two-dimensionally perfused flow chamber designs (figure 1(A)) and static culture conditions, respectively.

The MOTiF biochip consists of an upper and a lower flow chamber horizontally separated by a microporous PET membrane (figure 1(B)). The membrane acts as culture area for ECs. The integrated pores of 8 $\mu$m diameter allow basal perfusion and medium exchange to cultured EC layers through a lower perfusion channel, and in parallel apical perfusion via a separate upper perfusion channel (figures 1(B) and (C)). Dependent on the maximum local Reynolds numbers and Dean numbers above 50 in the inflow region, the formation and downstream propagation of Dean vortices can be expected. These fluid structures may superpose the laminar profile in the capillary slit at the endothelial layer resulting in non-predictable local shear stress variations in this zone. This effect has been considered in the design of the geometry of the vertical inflow region. Therefore, the cylindrical inflow was rounded in a direction-dependent way in order to increase the characteristic radius of the curvature in this region and secondly to decrease the average fluid velocity in this region. The geometry of the MOTiF biochip cavity generates laminar flow conditions during EC layer perfusion as verified by CFD analyses. CFD was calculated on the basis of measured contact angles for EC Medium with the bulk wall that has been treated with oxygen plasma for reducing hydrophobicity. Contact angle between flow medium and oxygen plasma-treated bulk wall was 43° ± 2° (supplementary figure 1(A)) and with the EC layer seeded on the membrane of the MOTiF biochip at 22° ± 2°, (supplementary figure 1(B)). CFD simulation based on these contact angels revealed that the formation of bubbles and turbulent flow on the channel inlet is prevented under these conditions. Filling characteristics in the inflow region of the main

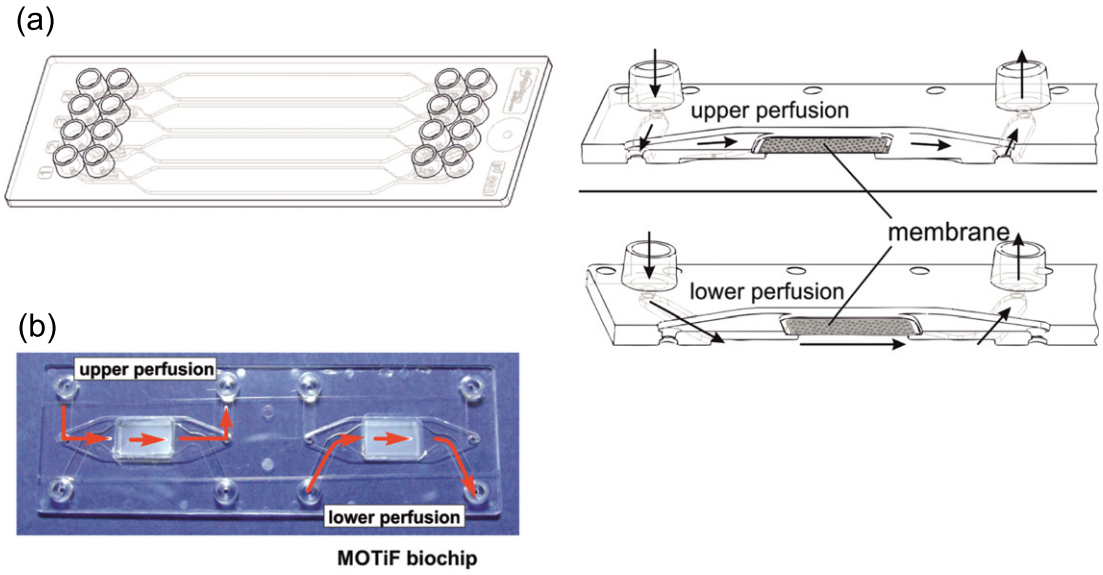


**Figure 1.** *2D Flow Chamber and MOTiF biochip design.* (A) Design of two-dimensionally perfused flow chambers. (B) MOTiF biochips contain two cavities, each comprising an integrated membrane serving as cell culture area. Cells cultured on the membrane are perfusable independently from both the apical or basal side through upward directed (upper perfusion) and downward directed (lower perfusion) channels. (B) Prototype of MOTiF biochips produced by injection molding with cyclic olefin polymers with welded membrane of polyethylene terephthalate.

chamber for the exchange of air by aqueous medium was investigated for surface contact angles in the range between 15 and 105° with a contact angle stepping of 15°. Bubble free exchange of the air by aqueous medium was observed for contact angles below 60°. At higher contact angle configurations an air bubble was formed in the pocket between the end of the top microchannel and the junction of the cylindrical inflow channel into the main channel (video 1). The same analysis has been performed for the exchange of air by aqueous medium for the outlet region of the main chamber. In this case, air exchange by aqueous buffer without remaining air bubbles was observed for contact angles below 75° (video 2). The complete fluid exchange and interface evolution for the main chamber was analyzed in the third simulation for the targeted contact angle configuration of the chip wall material of 82° and the membrane section with a contact angle of 22°. The contact line of the interface to the membrane precedes the interface contact line to the channel walls. The interface contact lines are orthogonal to the fluid transport direction. No tendency for inclusion air bubble formation is observed (video 3). In the video sequence the outflow section was not included since this aspect is always covered by the results of the outflow fluid exchange characteristics simulation.

In a first step we studied growth and vitality of endothelial layers on the chips under static and dynamic culture conditions. We used COC as bulk material for molding of two-dimensionally perfused flow chambers as well as MOTiF biochips in order to enable a direct comparison between both chip designs and to prevent polymer-related bias in the obtained results. To distinguish between the specific effects of continuous medium exchange and mechano-transduced effects of shear stress, we compared endothelial layers under low shear stress of 0.7 dyn $cm^{-2}$ with only minimal flow related mechanical stimulation, and high shear stress with 10 dyn $cm^{-2}$. The chosen high shear stress rate corresponds to the human *in vivo* situation in larger arteries and venules and represents the mean shear stress rate of common human carotid artery (Cheng *et al* 2007). ECs exhibit the typical cobblestone shape in static cell culture whereas in dynamic cell culture under perfusion the shear stress induces adaption within 24 h detectable as elongation of EC along the flow direction (figure 2(A)). Typical percentage of vital ECs under all culture conditions was above 97% as verified by calcein-AM staining (figure 2(B)) and flow cytometry (data not shown). ECs were characterized based on their morphology using the CSI. A CSI of 1 describes a circle and CSI of 0 describes a line. Although we observed no differences of ECs cultured in flow chambers and MOTiF biochips under low shear stress conditions, an improved adaption to high shear stress was detectable for ECs cultured in MOTiF biochips in respect to cell elongation and an increased cell density compared to flow chamber culture was detectable. Stimulation of ECs with high shear stress even reduced cell density in endothelial layers cultured in two-dimensionally perfused flow chambers (figures 2(C) and (D)).

Dynamic cell culture is known to mediate cytoskeleton rearrangements within ECs in response to shear stress (Malek and Izumo 1996). We therefore investigated endothelial actin microfilament organization under static conditions and after adaption of ECs to

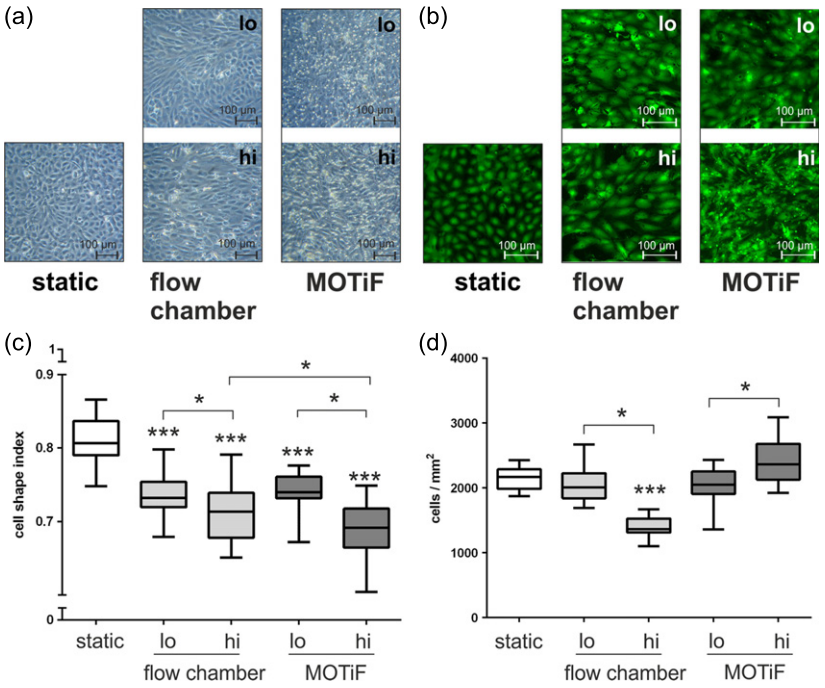


**Figure 2.** *Morphology and vitality of EC.* (A) Bright field images of EC cultured under static and dynamic conditions (lo: low shear stress, hi: high shear stress). (B) Viability staining of ECs with calcein-AM (C) cell density. (D) * $p < 0.05$; *** $p < 0.001$ versus static or between conditions as indicated (Student's t-test).

flow conditions within two-dimensionally perfused flow chambers and MOTiF biochips. Z-stack imaging of EC layers illustrates that endothelial layers within MOTiF biochips exhibit an increased mono-cell-layer thickness compared to corresponding conditions in flow chambers or static culture, respectively. Increased cell heights and densities were found associated with an intensified cytoskeleton remodeling, increased expression of F-actin and the formation of prominent stress fibers (figures 3(A) and (B)). F-actin fiber content correlated positively with increasing shear stress. In addition, endothelial F-actin expression was found significantly increased by MOTiF biochip culture compared to other culture conditions (figure 3(C)). In agreement with previous reports (Galbusera *et al* 1997), we observed increasing protein levels of vWF that correlated with the intensity of shear stress stimulation. Endothelial layers cultured in MOTiF biochips showed a significantly increased expression of vWF and a unique accumulation and intracellular localization of Weibel–Palade bodies (WPB) along with the appearance of extracellular patches and formation of vWF macrofilamentous strings (figures 3(D) and (E)). Similar to vWF we found an elevated expression of PECAM-1 on EC layers cultured within MOTiF biochips. Our observation that increased levels of vWF and PECAM-1 were predominantly found on areas of the culture membrane with a high pore density (figure 4(A)), supports the idea that apical and basal perfusion within MOTiF biochips not only improve supply of cell layers with nutritional culture medium but also favors rapid adaption of ECs to flow culture conditions.

The MOTiF biochips further provide the possibility to perform permeability assays under flow conditions. PECAM-1 and zonula occludens-1 (ZO-1) are critical regulators of endothelial permeability and associated pathophysiology (Harhaj and Antonetti 2004). We found elevated expression levels of PECAM-1 (figures 4(B) and (C)) and ZO-1 (figures 4(D) and (E)) on endothelial layers correlating with increasing shear stress stimulation (figure 4(E)). Flow-based permeability assays using FITC-labeled 40 kDa dextran revealed that EC layers cultured with high shear stress stimulation formed a tighter cell layer compared to low shear stress stimulation (figure 4(G)). It has been shown that treatment of EC layers with the proinflammatory cytokines TNF$\alpha$ and IFN$\gamma$ mediated a loss in barrier function (Lopez-Ramirez *et al* 2012). In agreement with these observations we found a significant elongation of cell morphology (figure 4(F)) upon treatment with TNF$\alpha$/IFN$\gamma$ that was further accompanied with a nearly complete breakdown of PECAM-1 and ZO-1 protein expression (figures 4(B)–(E)). The disintegration of cell connective proteins in consequence resulted in an increased permeability for dextran and breakdown of endothelial barrier function (figure 4(G)).

Inflammation within the vascular system not only involves leakage of endothelial layers but also mediates active recruitment of immune cells from the circulation depending on the interaction with CAM proteins. We therefore characterized endothelial layers in

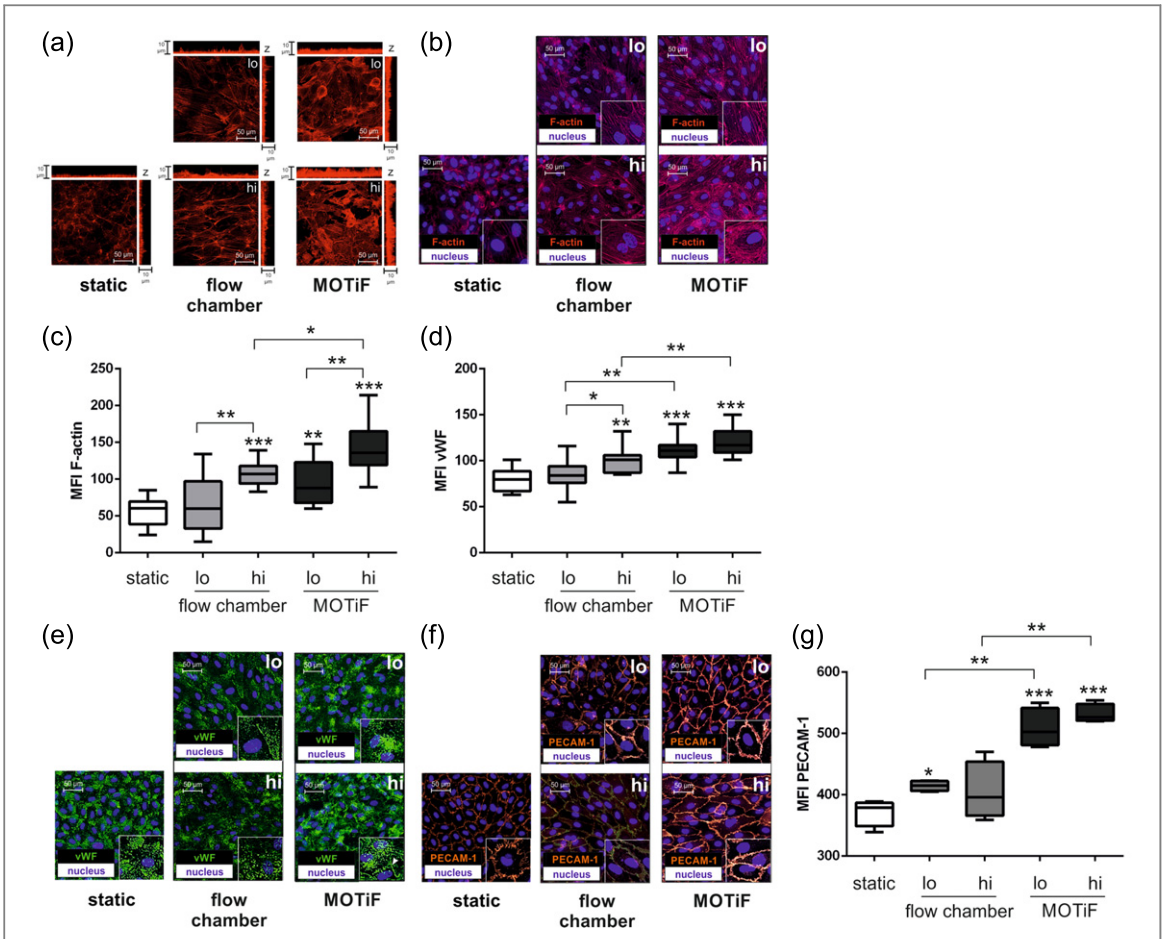


**Figure 3.** *Adaption of endothelial layers to shear stress.* F-actin arrangement and cytoskeleton remodeling visualized by (A) confocal Z-stack imaging and (B) two-dimensional immunofluorescence microscopy. Quantification of (C) actin and (D) vWF expression. (E) Expression of vWF. (F) Visualization and (G) quantification of PECAM-1 expression. * $p < 0.05$; ** $p < 0.01$, *** $p < 0.001$ versus static or between conditions as indicated (one-way ANOVA with Tukey's multiple testing comparison).With Tukey's multiple testing comparison * $p < 0.05$; ** $p < 0.01$, *** $p < 0.001$ compared to static or between indicated conditions.

MOTiF biochips for their cell surface expression of ICAM-1, VCAM-1 and E-selectin in response to pro-inflammatory TNF$\alpha$ stimulation. Without cytokine stimulation ICAM-1 expression was found up-regulated only under high shear stress conditions, whereas VCAM-1 expression declined under low as well as high shear stress conditions in MOTiF biochips compared to static cell culture. Expression of E-selectin was not effected by shear stress in the absence of cytokine stimulation. However, when cells were cultured under flow conditions, expression of all three CAMs declined in response to TNF$\alpha$ stimulation compared to static conditions (figures 5(A)–(C)). Functional relevance of altered CAM expression was tested by flow-based adhesion assays. Fluorescence-labeled THP-1 cells were continuously perfused through the upper channel of MOTiF biochips thereby overflowing the apical site of the EC layer equivalent to the lumen of a blood vessel. Simultaneously to THP-1 incubation with the endothelial layer, TNF$\alpha$ was applied through the lower perfusion channel. TNF$\alpha$ treatment activated ECs and mediated a significantly increased proportion of adhesive THP-1 cells under static and dynamic culture conditions (figures 5(D)). Highest amounts of adhesive THP-1 cells were found under static culture conditions. Within 30 min, THP-1 cells already formed filopodia on the endothelial layer that were not observed in the dynamic cell culture even with low shear stress stimulation (supplementary figure 1(C)). Furthermore, the number of THP-1 cells interacting with unstimulated as wells as TNF$\alpha$-activated endothelial layers decreased with increasing shear stress.

## Discussion

The development of cell culture technologies that better mimic the *in vivo* context for specific cell types are of great value for a better understanding of signaling pathways, the development of therapeutic strategies and for toxicity studies. This is mainly a consequence of the possibility to control experimental conditions much better, at least for proof of principle studies, than it is possible in living animals. As reported previously by other groups ECs exhibit remarkable changes in cell morphology when adapted to flow conditions (Levesque and Nerem 1985, Girard

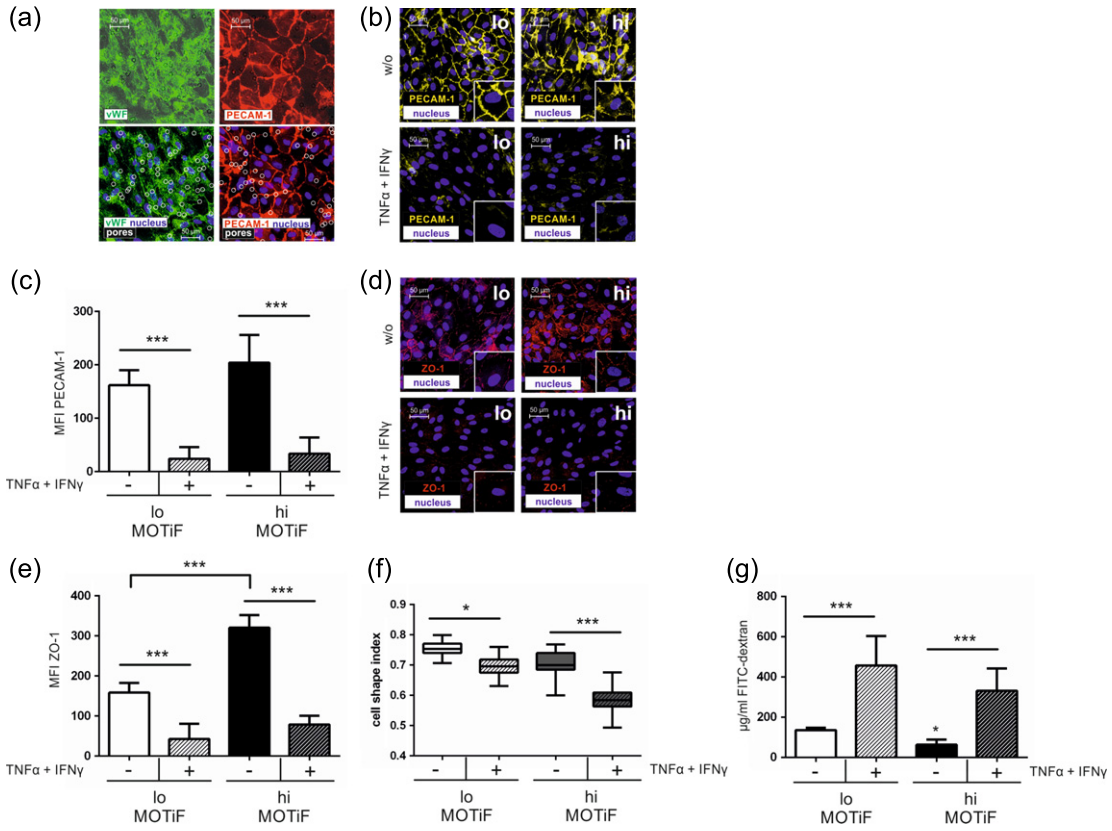


**Figure 4.** *Expression of vWF, PECAM-1 and ZO-1 in ECs cultured in MOTiF biochips.* (A) Expression of vWF and PECAM-1 in dependence of membrane pore density. For visualization and comparison purposes pores were marked in the lower images. (B) and (D) Expression of PECAM-1 (B) and ZO-1 (D) in dependence of shear stress and TNF$\alpha$/IFN$\gamma$ treatment in ECs cultured in MOTiF biochips. Quantification of PECAM-1 (C) and ZO-1 (E) expression in ECs cultured in MOTiF biochips. (F) Cell shape index. (G) Permeability of endothelial layers for 40 kDa FITC-labeled dextan. * $p < 0.05$; ** $p < 0.01$, *** $p < 0.001$ between conditions as indicated (Student's t-test).

and Nerem 1995). To ensure the best possible comparability and transferability between *in vitro* and *in vivo* studies, critical *in vitro* cell culture parameters such as the application of physiological shear stress and optimal perfusion conditions of the cells layers have to be taken into account. Therefore, flow chamber systems are being used more frequently for *in vitro* studies on EC biology instead of static cell culture conditions that lack the option to apply mechano-stimulatory effects. Although two-dimensionally perfused flow chambers provide an improved nutrition supply compared to static culture and allow the application of physiological shear stress these devices do not implement effects induced by flow-based permeability or transmigration. Further, cell culture within conventional dishes as well as two-dimensionally perfused flow chambers mostly includes growth of adherent cells on a tight and inflexible plastic substrate that prevents perfusion of the basal side of the cell membrane and limits nutrition supply and dynamic removal of cellular metabolites and catabolites. We therefore developed the MOTiF biochip design that offers improved perfusion conditions for the EC layers. Due to the option of stimulation with dynamically adjustable gradient concentrations during permeability or adherence/transmigration experiments from different cell membrane sides, the immune cell recruitment and modulation of endothelial permeability in response to cytokine stimulation from different luminal or basal derived sources can be investigated separately or in parallel. To characterize the MOTiF design for culture of endothelial layers we compared ECs under dynamic culture within MOTiF biochips in respect to viability, adaption to flow conditions and expression of endothelial marker proteins with static and dynamic culture conditions in two-dimensionally perfused flow chambers, respectively.

Inhomogeneous aggregation of EC cultured within MOTiF biochips could possibly influence flow dynamics across the membrane. However microscopic analysis revealed the formation of a tight, confluent and homogenous EC layer during culture in MOTiF biochips and a disturbed flow through inhomogeneous cell aggregation was not observed. ECs adapted to flow conditions in established flow chambers as well as in MOTiF biochips within 24 h. This became apparent by a change in cell morphology compared to static cell culture. In addition, ECs cultured in MOTiF biochips revealed an intensive modulation of

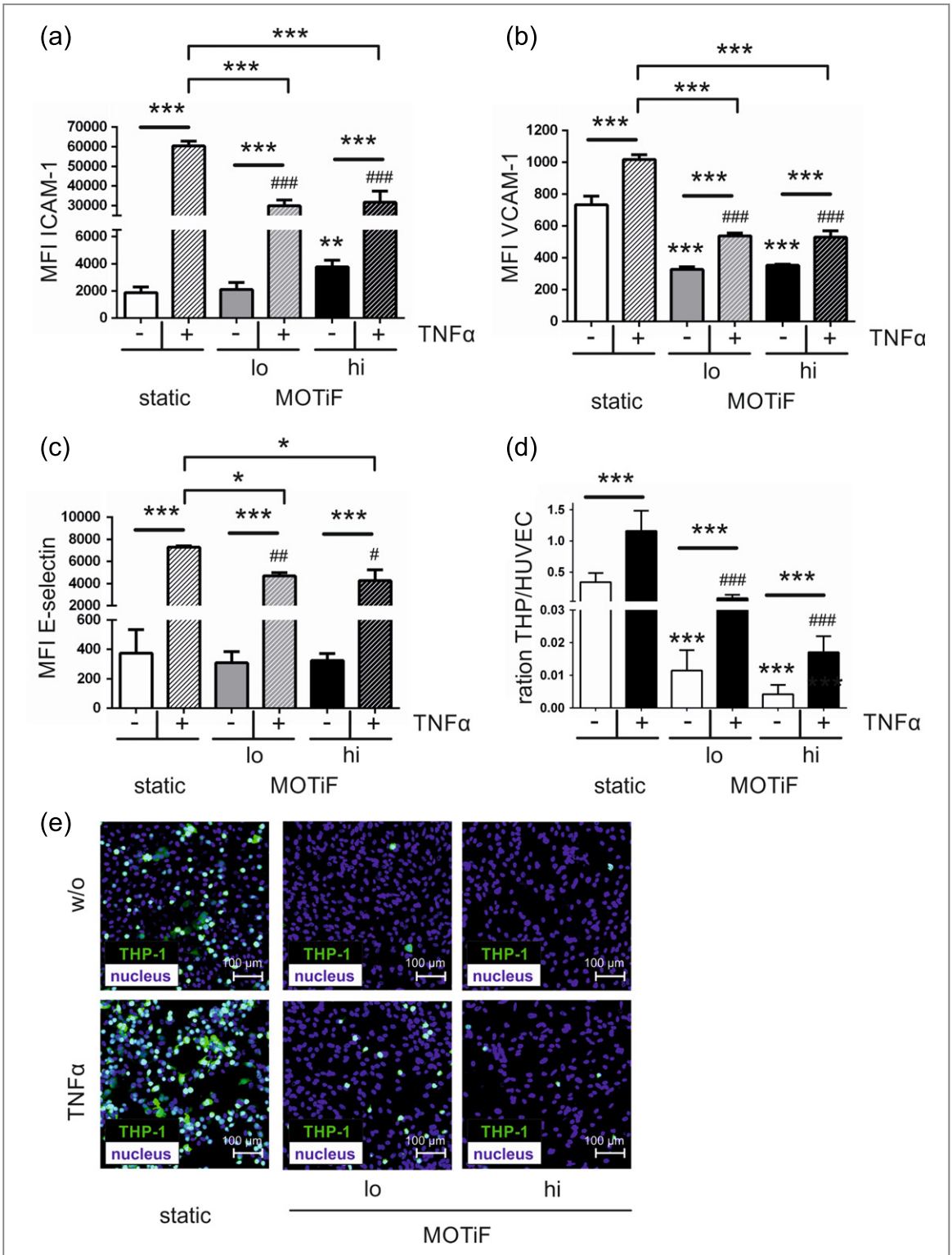


**Figure 5.** *Expression of endothelial CAMs and adhesion of THP-1 lymphocytes to ECs cultured in MOTiF biochips.* Expression of (A) ICAM-1, (B) VCAM-1, (C) E-selectin in ECs cultured in MOTiF biochips. (D)–(E) Adherent fluorescence-labeled THP-1 cells on HUVEC cell layer. (D) Ratio of adherent THP-1 cells to confluent EC. (E) Fluorescence microscopic images of adherent THP-1 to endothelial layer. * $p < 0.05$; ** $p < 0.01$, *** $p < 0.001$ between conditions as indicated (Student's t-test).

the cytoskeleton in response to flow and exhibited an increased cell height corresponding to enhanced polarity. The remodeling of the cytoskeleton was even more prominent in the MOTiF biochips when compared with standard flow chambers with identical shear stress application. Remodeling of the cytoskeleton in response to force from outside is induced by the generation of signals to the inside of a cell which subsequently induces the reorganization of the cytoskeleton and thereby reinforces the strength of cell attachment (Zhao *et al* 1995).

In addition, we observed that the expression of vWF was increased in the endothelial layers when grown in the MOTiF biochips. However, expression of

vWF was enhanced independently from shear stress stimulation within MOTiF biochips and was significantly increased when compared to two-dimensional flow chamber perfusion. Strongest expression of vWF was detectable in MOTiF biochips within areas of high pore-density on the membrane allowing improved basal medium perfusion. The impact of improved culture conditions also became apparent during the analysis of the cellular distribution of vWF on ECs in flow chambers and MOTiF biochips. Recently, multigranular exocytosis of vWF has been proposed to be a significant mode of exocytosis in which WPBs coalesce into a 'secretory pod' before fusing with the plasma membrane (Valentijn *et al* 2010). In ECs, the formation of secretory pods facilitates vWF string formation by accumulating the content of multiple WPBs before their release. The unique intracellular distribution of vWF within ECs cultured in MOTiF biochips shows remarkable morphological similarities with these secretory pods, and vWF macrofilament secretion colocalizes with these structures. The vWF string formation is dependent on neutral extracellular pH and is impaired if the pH within the WPBs is increased e.g. by pretreatment with monensin, which causes the disappearance of vWF strings (Valentijn *et al* 2010). Improved perfusion conditions in MOTiF biochips might thus contribute to a stable neutral extracellular pH thereby facilitating vWF string secretion. Exocytosis of vWF also depends on the interaction of WPBs with microtubules and actin cytoskeleton (Manneville *et al* 2003). Extensive remodeling as observed in MOTiF biochips assumed to contribute to increased vWF secretion. In addition exocytosis of WPBs is regulated by hypertensive stretch through VEGF-receptor 2 (VEGFR2) signaling pathways. In contrast to ECs cultured within two-dimensionally perfused flow chambers where cells are attached to an inflexible culture area, mechanical forces to endothelial layers can be generated when grown on the free-hanging membrane within MOTiF biochips. We speculate that flow conditions in the dynamic culture induce a limited stretching of the PET membrane and the cultured endothelial layer thereon. Stretch of the endothelium is known to trigger a rapid release of vWF strings from WPBs (Xiong *et al* 2013) that have been shown to remain associated with cells for a considerable time (Michaux *et al* 2006, Huang *et al* 2008). These vWF strings are a physiological requirement in the healthy endothelium and known to prevent coagulopathy and impaired wound healing (Federici and Mannucci 2007).

Furthermore, multigranular exocytosis of vWF strings has been shown to constitute an important pathway for the regulated release of VWF by vascular ECs (Valentijn *et al* 2010). vWF string formation and secretion was not observed under static cell culture conditions and only to a limited extent in two-dimensionally perfused flow chambers. In this context we want to note, that ultra-large von Willebrand fibers that are formed under pathophysiological conditions from vWF strings were reported to be important in the initial pathogenic step of *S.aureus*-induced endocarditis in patients with an apparently intact endothelium (Pappelbaum *et al* 2013). Although we do not know the exact mechanisms by which vWF string formation is induced in MOTiF biochips we suppose that endothelial layers obtained therein might be an interesting *in vitro* model for studies on immune cell interactions with EC layers under improved perfusion conditions and with new methodical possibilities compared to two-dimensionally perfused flow chambers.

In regard to immune cell interactions with ECs the maintenance and regulation of endothelial barrier function is one of the most imported tasks at the vessel wall. PECAM-1 is known to be a critical regulator of immune cell trafficking and maintenance of EC junctional integrity (Privratsky *et al* 2010). PECAM-1 is known to be protective in ECs during inflammation due to its ability to inhibit pro-inflammatory cytokine signaling and maintaining of vascular integrity (Carrithers *et al* 2005, Maas *et al* 2005, Privratsky *et al* 2010). Furthermore, ZO-1 which connects to and stabilizes endothelial tight junctions within lateral cell-cell contact and thereby contributes to endothelial barrier function (Chattopadhyay *et al* 2014) was found up-regulated by high shear stress in ECs cultured within MOTiF biochips. Thus, increased expression of PECAM-1 as well as ZO-1 likely contributes to improved barrier function observed in response to high shear stress stimulation within MOTiF biochips. In addition, also the prolonged lateral cell–cell contacts of thickened EC monolayers (mediated by amplified cytoskeleton rearrangement) further contribute to elevated barrier function of EC layers stimulated with high shear stress. Similar observations were made with microfluidic models using kidney epithelial cells that responded to fluid shear stress by increasing their cell height and actin cytoskeleton rearrangement, also resulting in the formation of tighter cell layers (Jang *et al* 2011, Jang *et al* 2013). During inflammation PECAM-1 is redistributed and down-regulated from lateral junctions (Stewart *et al* 1996) resulting in a loos of endothelial barrier function (Fernández-Martín *et al* 2012). We reproduced this phenomenon by basal application of proinflammatory cytokines TNF$\alpha$ and IFN$\gamma$ to EC layers, demonstrating the feasibility of MOTiF biochips for usage in flow-based permeability assays. The basal stimulation of ECs with cytokines in the dynamic cell culture was associated with an elongation of stimulated ECs. It was recently shown that EC activation by TNF$\alpha$ is not only accompanied with augmented cell elongation under flow conditions but also with a dynamic shifts of the cytoskeleton and reduced cell stiffness (Stroka *et al* 2012). Thus, the observed leakage of endothelial layers in response to TNF$\alpha$/IFN$\gamma$ treatment is likely mediated by loos of PECAM-1 and ZO-1 expression combined with reduced cytoskeleton stiffness.

Activation of ECs also includes alterations in CAM expression. EC layers in MOTiF biochips exhibited a characteristic CAM expression profile in response to shear stress. In accordance with previous reports ECs adapt to high shear stress by up-regulation of ICAM-1 expression and down-regulation of VCAM-1 (Morigi *et al* 1995, Tsao *et al* 1996). Concordant with this we observed a diminished expression of ICAM-1, VCAM-1 and E-selectin in the dynamic cell culture in MOTiF biochips under low as well as high shear stress conditions in response to TNF$\alpha$ treatment compared to static culture. Down-regulation of CAM expression has been shown to be mediated by release of nitric oxide by ECs in response to shear stress (De Caterina *et al* 1995). Furthermore, laminar shear stress attenuates the expression of E-selectin and VCAM-1 in response to TNF$\alpha$ modulation by NF-$\kappa$B-dependent signaling pathways (Chiu *et al* 2004, Partridge *et al* 2007).

However, in these studies the authors show an increased ICAM-1 expression in response to TNF$\alpha$ by shear stress whereas in our studies a down-regulation of ICAM-1 expression after TNF$\alpha$ treatment during low as well as high shear stress stimulation was detectable. We speculate that the observed differences might be due to different stimulation times used. Partridge *et al* and Chiu *et al* stimulated HUVEC with TNF$\alpha$ for 2 h and 4 h, respectively. In our setting endothelial layers were stimulated during the entire 24 h shear stress stimulation (Chiu *et al* 2004, Partridge *et al* 2007).

We have shown that endothelial layers cultured in MOTiF biochips exhibit an improved expression of EC marker proteins. We used different flow rates in perfusion experiments with two-dimensional and 3D perfusion. Generally, increasing flow rate resulted in higher cell density and expression of EC markers irrespective of the chip design and material used. However, additional basal perfusion in MOTiF chips had higher impact on EC density and marker expression than apical perfusion alone at identical flow rates. From this we conclude that improved basal perfusion of cell layers is beneficial to EC cell culture.

It is reasonable that rigidity of the substrate has effects on cell physiology. We observed increased expression of actin, vWF and PECAM-1 compared to solely apical perfusion already by low basal shear stress perfusion in MOTiF biochips. These low shear stress conditions are considered to not result in significant stretching of the membrane and thereby should not induce additional mechanostimulatory effects from the basal side. However, by increasing basal flow rate in MOTiF chips we observed a further improvement of cellular parameters compared to conditions with only apical perfusion. Under these conditions an additional mechanical stimulation of ECs through stretching of the membrane surface might have a relevant effect, thus further contributing to improved cell function. Although we cannot explain the underlying mechanism, we can conclude that enhanced perfusion in MOTiF biochips significantly contributes to the improved EC function observed under dynamic flow culture conditions.

Expression and cellular distribution of vWF in MOTiF biochips share similarities to the *in vivo* state that are not observed in two-dimensionally perfused flow chambers or under static culture conditions. In addition, the MOTiF biochips allow simultaneous perfusion through both microchannels with dynamically adjustable flow rates and flow modes such as oscillatory or continuous flow that can be individually adjusted to the respective microchannel and side of cell layer perfusion. Moreover, MOTiF chips are suitable for advanced studies on immune cell interaction with adherent cell layers under flow conditions. The MOTiF biochips device allows the dynamic adjustment of substance concentrations during perfusion and basal stimulation of MOTiF biochips embedded cell layers together with a simultaneous application of suspension cells overflowing and interacting with the adherent cell layer. The MOTiF biochips design thus combines the advantages of the widely used cell culture filter membrane inserts for culturing polarized cell types such as ECs thereby enabling studies of transport, secretion, absorption and permeability combined with the features of flow chamber systems offering flow-based permeability and adhesion/transmigration assays.

We have shown that the MOTiF biochips represent a valuable tool for dynamic cell culture with improved perfusion conditions that overcome some limitations of two-dimensionally perfused flow chambers. One of the most important limitations of 3D tissue culture even under dynamic conditions within two-dimensionally perfused flow chambers is the sufficient supply of cells with nutrients and oxygen as well as the removal of unwanted cell metabolites/catabolites. This is mainly due to increased diffusion ranges from the apical tissue side to the bottom of the cell culture device throughout the tissue as simultaneous apical and basal perfusion is not possible in these devices. The MOTiF biochip design allows individually adjustable flow conditions for both, upper and lower microdevice channels and an overall improved perfusion condition for cell layers when compared to static cell culture or two-dimensionally perfused flow chambers. Thus MOTiF biochips might also be a suitable device for long-term 3D cell culture approaches. Studies are currently underway to elucidate the potential of the MOTiF biochips design for long-term culture of e.g. multilayered 3D tissues.

## Acknowledgments

We are grateful to the excellent technical work of Maria Franke and Margot Voigt. We thank the team of the Placenta Laboratory of the Jena University Hospital for supplying umbilical cords for HUVEC isolation.

The authors would further like to acknowledge support of this work by 2011 VF 0005 grant of the Thüringer Aufbaubank. This work was further supported by the FK 3 1329-470 grant from the Federal Agency on Risk Assessment and in part by the Federal Ministry of Education and Research (BMBF), Germany, FKZ: 01EO1002.

## References

Berthier E, Young E W K and Beebe D 2012 Engineers are from PDMS-land, biologists are from polystyrenia *Lab Chip* **12** 1224–37

Carrithers M, Tandon S, Canosa S, Michaud M, Graesser D and Madri J A 2005 Enhanced susceptibility to endotoxic shock and impaired STAT3 signaling in CD31-deficient mice *Am. J. Pathol.* **166** 185–96

Chattopadhyay R, Dyukova E, Singh N K, Ohba M, Mobley J A and Rao G N 2014 Vascular endothelial tight junctions and barrier function are disrupted by 15(S)-hydroxyeicosatetraenoic acid partly via protein kinase C $\varepsilon$-mediated zona occludens-1 phosphorylation at threonine 770/772 *J. Biol. Chem.* **289** 3148–63

Cheng C *et al* 2007 Large variations in absolute wall shear stress levels within one species and between species *Atherosclerosis* **195** 225–35

Chiu J-J, Lee P-L, Chen C-N, Lee C-I, Chang S-F, Chen L-J, Lien S-C, Ko Y-C, Usami S and Chien S 2004 Shear stress increases ICAM-1 and decreases VCAM-1 and E-selectin expressions induced by tumor necrosis factor-[alpha] in endothelial cells *Arterioscler. Thromb. Vasc. Biol.* **24** 73–9

Davies P F 1995 Flow-mediated endothelial mechanotransduction *Physiol. Rev.* **75** 519–60

Davies P F, Reidy M A, Goode T B and Bowyer D E 1976 Scanning electron microscopy in the evaluation of endothelial integrity of the fatty lesion in atherosclerosis *Atherosclerosis* **25** 125–30

de Caterina R, Libby P, Peng H B, Thannickal V J, Rajavashisth T B, Gimbrone M A, Shin W S and Liao J K 1995 Nitric oxide decreases cytokine-induced endothelial activation. Nitric oxide selectively reduces endothelial expression of adhesion molecules and proinflammatory cytokines *J. Clin. Invest.* **96** 60–8

Eddington D T, Puccinelli J P and Beebe D J 2006 Thermal aging and reduced hydrophobic recovery of polydimethylsiloxane *Sensors Actuators* B **114** 170–2

El-Ali J, Sorger P K and Jensen K F 2006 Cells on chips *Nature* **442** 403–11

Federici A B and Mannucci P M 2007 Management of inherited von Willebrand disease in 2007 *Ann. Med.* **39** 346–58

Fernández-Martín L *et al* 2012 Crosstalk between reticular adherens junctions and platelet endothelial cell adhesion molecule-1 regulates endothelial barrier function *Arterioscler. Thromb. Vasc. Biol.* **32** e90–102

Flaherty J T, Pierce J E, Ferrans V J, Patel D J, Tucker W K and Fry D L 1972 Endothelial nuclear patterns in the canine arterial tree with particular reference to hemodynamic events *Circ. Res.* **30** 23–33

Galbusera M, Zoja C, Donadelli R, Paris S, Morigi M, Benigni A, Figliuzzi M, Remuzzi G and Remuzzi A 1997 Fluid shear stress modulates von Willebrand factor release from human vascular endothelium *Blood* **90** 1558–64

Geiger B, Bershadsky A, Pankov R and Yamada K M 2001 Transmembrane crosstalk between the extracellular matrix–cytoskeleton crosstalk *Nat. Rev. Mol. Cell Biol.* **2** 793–805

Geuzaine C and Remacle J-F 2009 Gmsh: a 3D finite element mesh generator with built-in pre- and post-processing facilities *Int. J. Numer. Methods Eng.* **79** 1309–31

Girard P R and Nerem R M 1995 Shear stress modulates endothelial cell morphology and F-actin organization through the regulation of focal adhesion-associated proteins *J. Cell. Physiol.* **163** 179–93

Goode T B, Davies P F, Reidy M A and Bowyer D E 1977 Aortic endothelial cell morphology observed in situ by scanning electron microscopy during atherogenesis in the rabbit *Atherosclerosis* **27** 235–51

Harhaj N S and Antonetti D A 2004 Regulation of tight junctions and loss of barrier function in pathophysiology *Int. J. Biochem. Cell Biol.* **36** 1206–37

Henderson A 2004 *The ParaView Guide: A Parallel Visualization Application* (Clifton Park, NY: Kitware) p 1

Huang R-H, Wang Y, Roth R, Yu X, Purvis A R, Heuser J E, Egelman E H and Sadler J E 2008 Assembly of Weibel–Palade body-like tubules from *N*-terminal domains of von Willebrand factor *Proc. Natl Acad. Sci. USA* **105** 482–7

Huh D, Kim H J, Fraser J P, Shea D E, Khan M, Bahinski A, Hamilton G A and Ingber D E 2013 Microfabrication of human organs-on-chips *Nat. Protocols* **8** 2135–57

Jaffe E A, Nachman R L, Becker C G and Minick C R 1973 Culture of human endothelial cells derived from umbilical veins. Identification by morphologic and immunologic criteria *J. Clin. Invest.* **52** 2745–56

Jang K-J, Cho H S, Kang D H, Bae W G, Kwon T-H and Suh K-Y 2011 Fluid-shear-stress-induced translocation of aquaporin-2 and reorganization of actin cytoskeleton in renal tubular epithelial cells *Integr. Biol.* **3** 134–41

Jang K-J, Mehr A P, Hamilton G A, McPartlin L A, Chung S, Suh K-Y and Ingber D E 2013 Human kidney proximal tubule-on-a-chip for drug transport and nephrotoxicity assessment *Integr. Biol.* **5** 1119–29

Kwei S, Stavrakis G, Takahas M, Taylor G, Folkman M J, Gimbrone M A J and García-Cardeña G 2004 Early adaptive responses of the vascular wall during venous arterialization in mice *Am. J. Pathol.* **164** 81–9

Levesque M J and Nerem R M 1985 The elongation and orientation of cultured endothelial cells in response to shear stress *J. Biomech. Eng.* **107** 341–7

Lopez-Ramirez M A, Fischer R, Torres-Badillo C C, Davies H A, Logan K, Pfizenmaier K, Male D K, Sharrack B and Romero I A 2012 Role of caspases in cytokine-induced barrier breakdown in human brain endothelial cells *J. Immunology* **189** 3130–9

Maas M, Stapleton M, Bergom C, Mattson D L, Newman D K and Newman P J 2005 Endothelial cell PECAM-1 confers protection against endotoxic shock *Am. J. Physiol. Heart Circ. Physiol.* **288** H159–64

Malek A M and Izumo S 1996 Mechanism of endothelial cell shape change and cytoskeletal remodeling in response to fluid shear stress *J. Cell. Sci.* **109** 713–26

Manneville J-B, Etienne-Manneville S, Skehel P, Carter T, Ogden D and Ferenczi M 2003 Interaction of the actin cytoskeleton with microtubules regulates secretory organelle movement near the plasma membrane in human endothelial cells *J. Cell. Sci.* **116** 3927–38

Michaux G, Abbitt K B, Collinson L M, Haberichter S L, Norman K E and Cutler D F 2006 The physiological function of von Willebrand's factor depends on its tubular storage in endothelial Weibel–Palade bodies *Dev. Cell* **10** 223–32

Morigi M, Zoja C, Figliuzzi M, Foppolo M, Micheletti G, Bontempelli M, Saronni M, Remuzzi G and Remuzzi A 1995 Fluid shear stress modulates surface expression of adhesion molecules by endothelial cells *Blood* **85** 1696–703

Nagel T, Resnick N, Atkinson W J, Dewey C F J and Gimbrone M A J 1994 Shear stress selectively upregulates intercellular adhesion molecule-1 expression in cultured human vascular endothelial cells *J. Clin. Invest.* **94** 885–91

Pappelbaum K I *et al* 2013 Ultralarge von Willebrand factor fibers mediate luminal *Staphylococcus aureus* adhesion to an intact endothelial cell layer under shear stress *Circulation* **128** 50–9

Partridge J *et al* 2007 Laminar shear stress acts as a switch to regulate divergent functions of NF-kappaB in endothelial cells *FASEB J.* **21** 3553–61

Privratsky J R, Newman D K and Newman P J 2010 PECAM-1: conflicts of interest in inflammation *Life Sci.* **87** 69–82

Ramadan Q et al 2013 NutriChip: nutrition analysis meets microfluidics *Lab Chip* **13** 196–203
Ramello C, Paullier P, Ould-Dris A, Monge M, Legallais C and Leclerc E 2011 Investigation into modification of mass transfer kinetics by acrolein in a renal biochip *Toxicology In Vitro* **25** 1123–31
Regehr K J, Domenech M, Koepsel J T, Carver K C, Ellison-Zelski S J, Murphy W L, Schuler L A, Alarid E T and Beebe D J 2009 Biological implications of polydimethylsiloxane-based microfluidic cell culture *Lab Chip* **9** 2132–9
Stewart R J, Kashour T S and Marsden P A 1996 Vascular endothelial platelet endothelial adhesion molecule-1 (PECAM-1) expression is decreased by TNF-alpha and IFN-gamma. Evidence for cytokine-induced destabilization of messenger ribonucleic acid transcripts in bovine endothelial cells *J. Immunology* **156** 1221–8
Stroka K M, Vaitkus J A and Aranda-Espinoza H 2012 Endothelial cells undergo morphological, biomechanical, and dynamic changes in response to tumor necrosis factor-$\alpha$ *Eur. Biophys. J.* **41** 939–47
Thuenauer R, Rodriguez-Boulan E and Römer W 2014 Microfluidic approaches for epithelial cell layer culture and characterisation *Analyst* **139** 3206–18
Toepke M W and Beebe D J 2006 PDMS absorption of small molecules and consequences in microfluidic applications *Lab Chip* **6** 1484–6
Traub O and Berk B C 1998 Laminar shear stress: mechanisms by which endothelial cells transduce an atheroprotective force *Arterioscler. Thromb. Vasc. Biol.* **18** 677–85
Tsao P S, Buitrago R, Chan J R and Cooke J P 1996 Fluid flow inhibits endothelial adhesiveness nitric oxide and transcriptional regulation of VCAM-1 *Circulation* **94** 1682–9
Tzima E, Irani-Tehrani M, Kiosses W B, Dejana E, Schultz D A, Engelhardt B, Cao G, DeLisser H and Schwartz M A 2005 A mechanosensory complex that mediates the endothelial cell response to fluid shear stress *Nature* **437** 426–31
Valentijn K M, van Driel L F, Mourik M J, Hendriks G-J, Arends T J, Koster A J and Valentijn J A 2010 Multigranular exocytosis of Weibel–Palade bodies in vascular endothelial cells *Blood* **116** 1807–16
van Midwoud P M, Janse A, Merema M T, Groothuis G M M and Verpoorte E 2012 Comparison of biocompatibility and adsorption properties of different plastics for advanced microfluidic cell and tissue culture models *Anal. Chem.* **84** 3938–44
Wang L, Zhang Z-L, Wdzieczak-Bakala J, Pang D-W, Liu J and Chen Y 2011 Patterning cells and shear flow conditions: convenient observation of endothelial cell remoulding, enhanced production of angiogenesis factors and drug response *Lab Chip* **11** 4235
Whitesides G M 2006 The origins and the future of microfluidics *Nature* **442** 368–73
Xiong Y et al 2013 Hypertensive stretch regulates endothelial exocytosis of Weibel–Palade bodies through VEGF receptor 2 signaling pathways *Cell Res.* **23** 820–34
Young E W K and Simmons C A 2010 Macro- and microscale fluid flow systems for endothelial cell biology *Lab Chip* **10** 143–60
Zhao S, Suciu A, Ziegler T, Moore J E, Bürki E, Meister J J and Brunner H R 1995 Synergistic effects of fluid shear stress and cyclic circumferential stretch on vascular endothelial cell morphology and cytoskeleton *Arterioscler. Thromb. Vasc. Biol.* **15** 1781–6